Magnetite Petrochemistry in Alaskan-type Ultramafic-Mafic Intrusions of British Columbia: Controls of Magmatic, Mineralization, Subsolidus, and Hydrothermal Processes

Ian R. Goan (UBC), James S. Scoates (UBC), Dejan Milidragovic (NRCan-GSC/UBC), Dylan W. Spence (UBC), James A. Nott (UBC), Graham T. Nixon (BCGS)

Natural Resources Canada / Ressources naturelles Canada
Canada
NSERC CRSNG
TGI Ore Systems

Recommended Citation: Goan, I.R., Scoates, J.S., Milidragovic, D., Spence, D.W., Nott, J.A., and Nixon, G.T., 2026. Magnetite petrochemistry in Alaskan-type ultramafic–mafic intrusions of British Columbia: Controls of magmatic, mineralization, subsolidus, and hydrothermal processes. British Columbia Ministry of Mining and Critical Minerals, British Columbia Geological Survey GeoFile 2026-04 (poster).

ABSTRACT

Magnetite (Fe_3O_4), a sensitive recorder of magmatic differentiation and subsolidus modification, has been utilized as an indicator mineral in ore-forming systems (e.g., Ni-Cu-PGE, Fe-Ti-V, porphyry, IOCG, skarn). This study investigates the trace element chemistry of magnetite, determined by both EPMA and LA-ICP-MS, from Late Triassic to Early Jurassic Alaskan-type ultramafic–mafic intrusions in British Columbia (Hickman, Polaris, Tulameen, Turnagain). In these intrusions, magnetite is a common accessory mineral (5–10 vol%) in clinopyroxenite and hornblendite, having crystallized primarily as an interstitial phase which was subsequently modified by variable subsolidus oxidation (e.g., pleonaste and ilmenite exsolutions) and fluid interaction. Compatible elements (e.g., Cr-Ni) trace magmatic evolution, where less-evolved magnetite in wehrlite and clinopyroxenite contains higher concentrations of these elements compared to more evolved magnetite in hornblendite. Segregation of an immiscible sulfide liquid in Turnagain, host to a large undeveloped Ni-sulfide deposit and Cu-PGE mineralization, is recorded by strongly Ni-depleted magnetite. Vanadium concentrations, a redox-sensitive element, vary little across the studied Alaskan-type intrusions, reflecting the relatively oxidized conditions of these magmatic systems. Several discrimination diagrams, commonly used to classify magnetite based on deposit type and mineralization potential, were compared in this study. Application to Alaskan-type intrusions highlights the importance of careful consideration of petrologic context, hydrothermal overprinting, and effects of sulfide saturation when utilizing magnetite discrimination diagrams. The results of this study demonstrate that magnetite petrochemistry is an effective tracer of magmatic and mineralization processes in primitive arc magmas and that these results can be broadly applied to magnetite-bearing systems globally.

MAGNETITE IN ALASKAN-TYPE INTRUSIONS

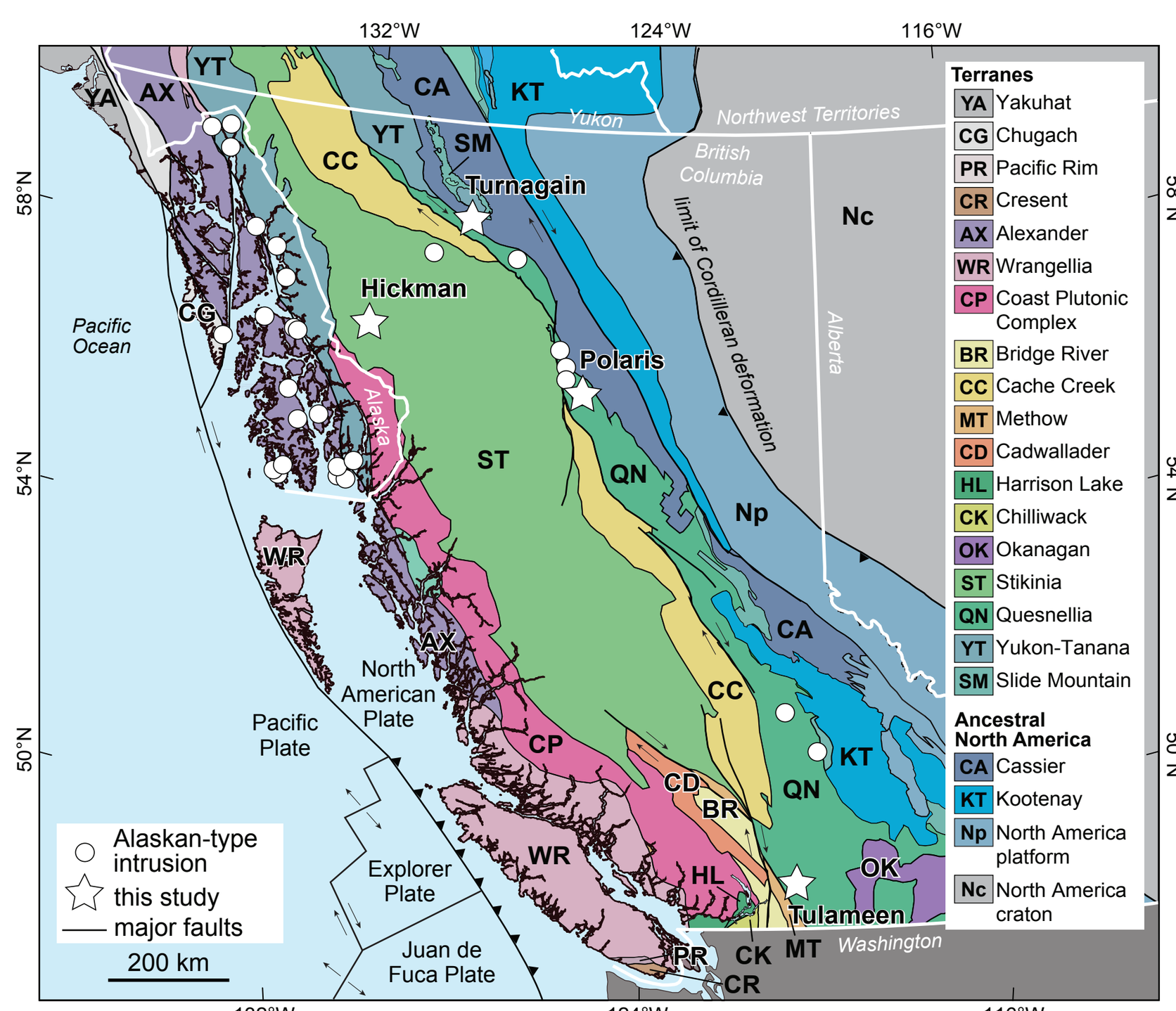

Fig. 1. Geological terrane map of the Canadian Cordillera (modified from Colpron & Nelson, 2011a) showing the distribution of Alaskan-type intrusions in British Columbia and the Alaskan Panhandle (after Himmelberg & Loney, 1995; Nixon et al., 1997). Stars represent locations of the four intrusions investigated in this study (Hickman, Polaris, Tulameen, Turnagain).

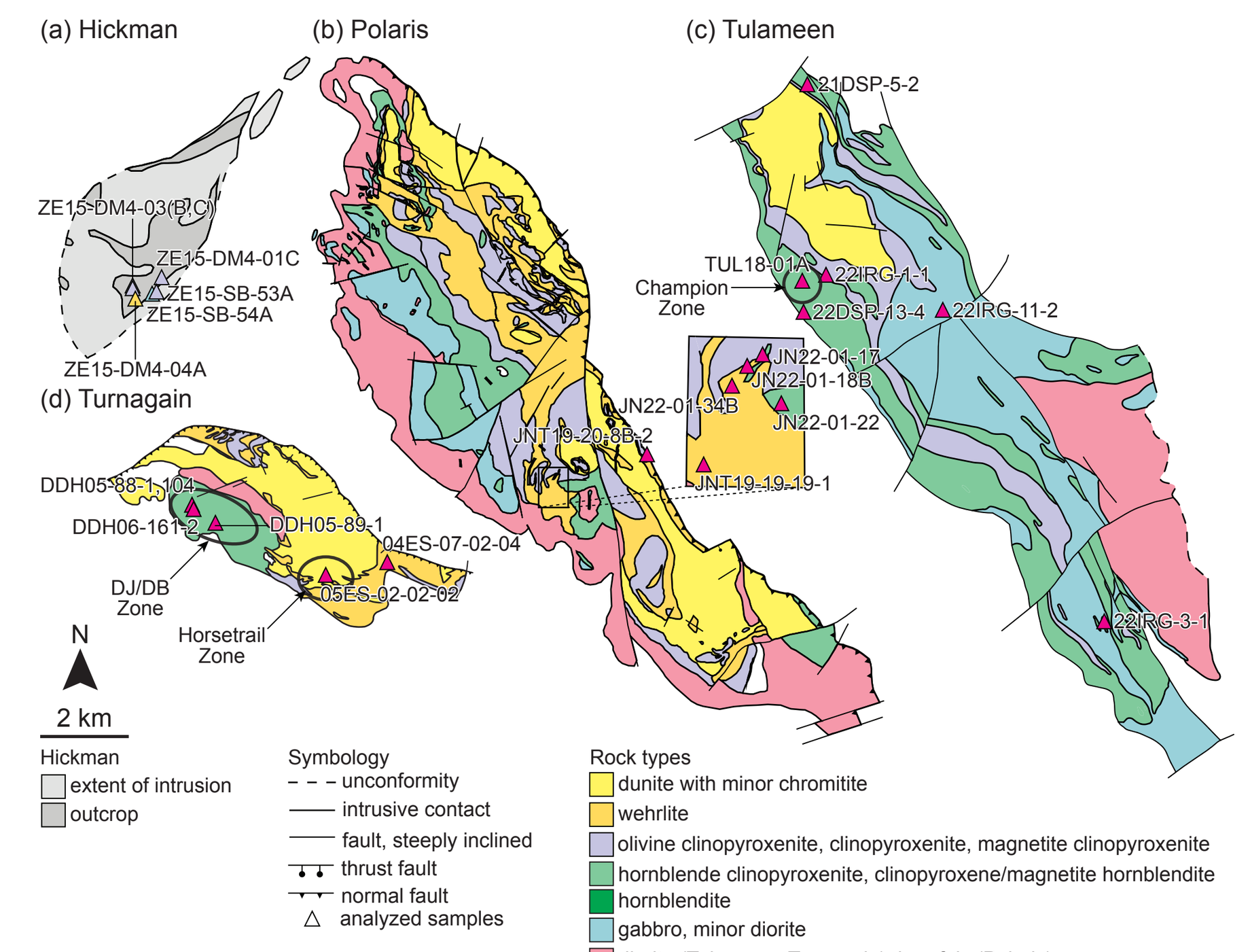

Fig. 2. Simplified geologic maps of the four Alaskan-type intrusions investigated in this study; all maps are at the same scale. (a) Hickman (adapted from Milidragovic et al., 2017). (b) Polaris (adapted from Nott et al., 2020b). (c) Tulameen (adapted from Nixon, 2018). (d) Turnagain (adapted from Nixon et al., 2019). Black ellipsoids represent the main magmatic sulfide occurrences at Tulameen (Cu-PGE Champion zone) and Turnagain (Cu-PGE DJ/DB and Ni Horsetrail zones). Magenta triangles show sample locations. Note that fill colors for Hickman samples correspond to rock type.

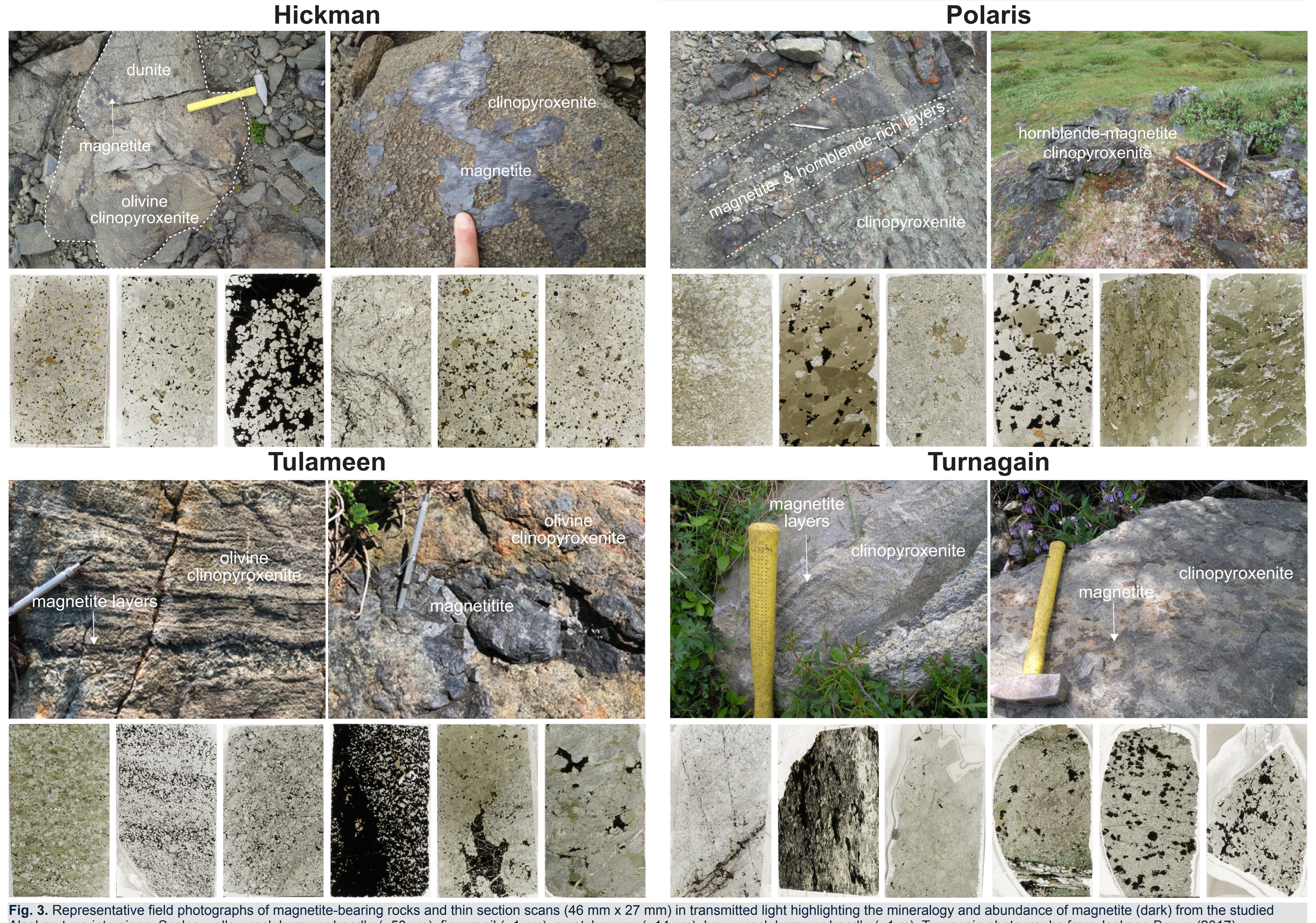

Fig. 3. Representative field photographs of magnetite-bearing rocks and thin section scans (46 mm x 27 mm) in transmitted light highlighting the mineralogy and abundance of magnetite (dark) from the studied Alaskan-type intrusions. Scales: yellow rock hammer handle (~50 cm), fingernail (~1 cm), scratcher pen (~14 cm), brown rock hammer handle (~1 m). Turnagain photographs from Jackson-Brown (2017).

MAGNETITE TEXTURES & ANALYTICAL TECHNIQUES

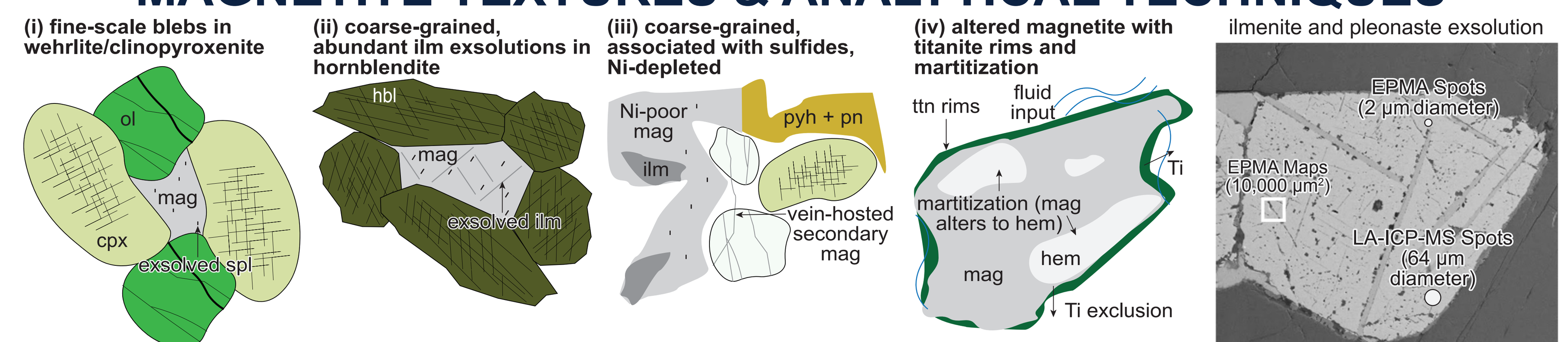

Fig. 4. Grain-scale sketches of textures highlighting key petrographic and geochemical variations of magnetite from Alaskan-type intrusions. Mineral abbreviations: cpx (clinopyroxene), hem (hematite), hbl (hornblende), ilm (ilmenite), mag (magnetite), ol (olivine), pn (pentlandite), pyh (pyrrhotite), spl (spinel), ttn (titanite).

PROCESSES RECORDED BY MAGNETITE PETROCHEMISTRY

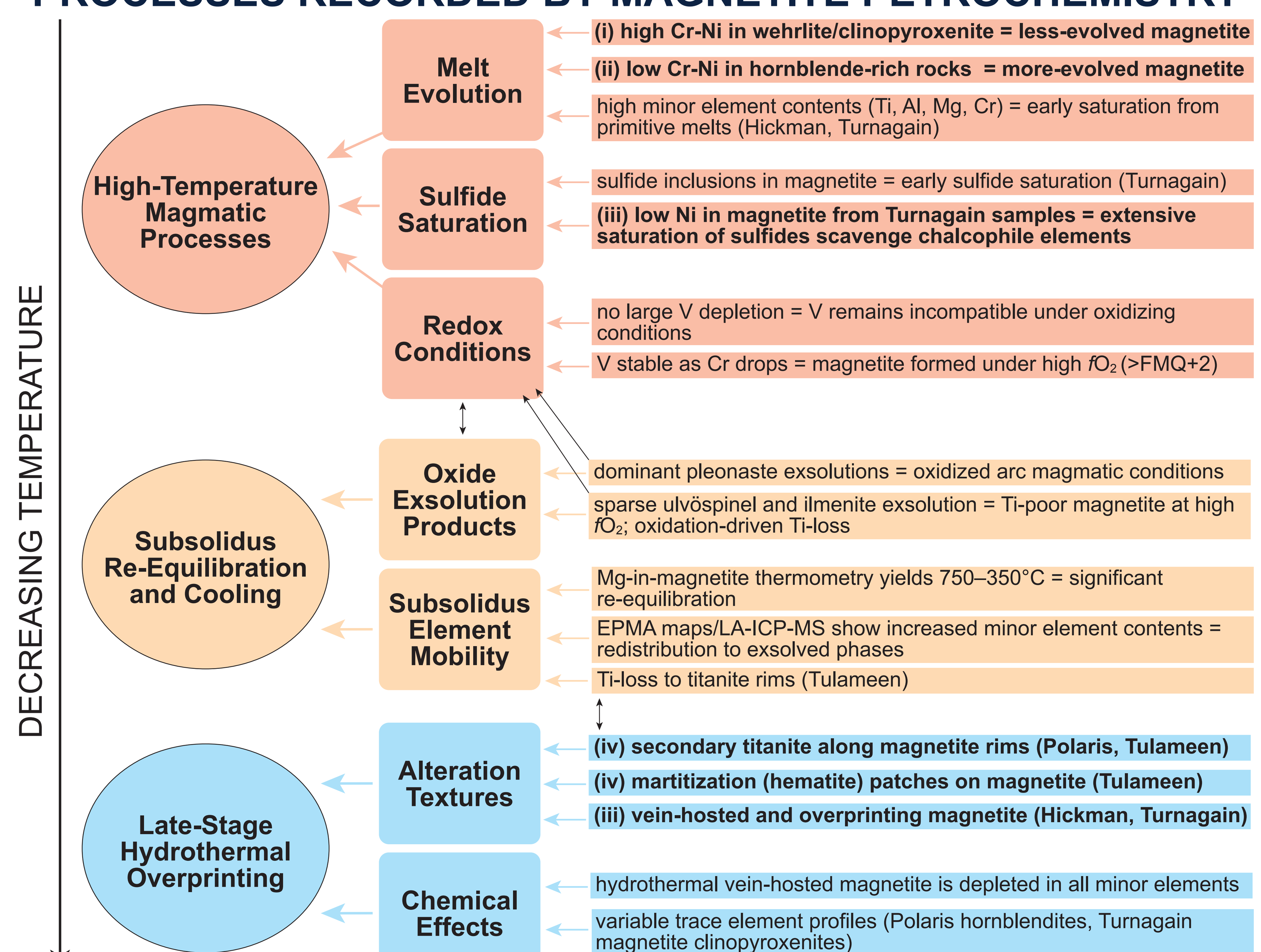

Fig. 5. Summary of processes highlighting key petrographic and geochemical variations of magnetite from Alaskan-type intrusions. The three colors represent high-temperature processes (red, magmatic crystallization ~990°C) to near- to subsolidus re-equilibration (yellow, ~700°C) and hydrothermal overprinting (blue, <700°C). Roman numerals are associated with the sketches of magnetite textures in Fig. 4.

MAGNETITE CHEMISTRY

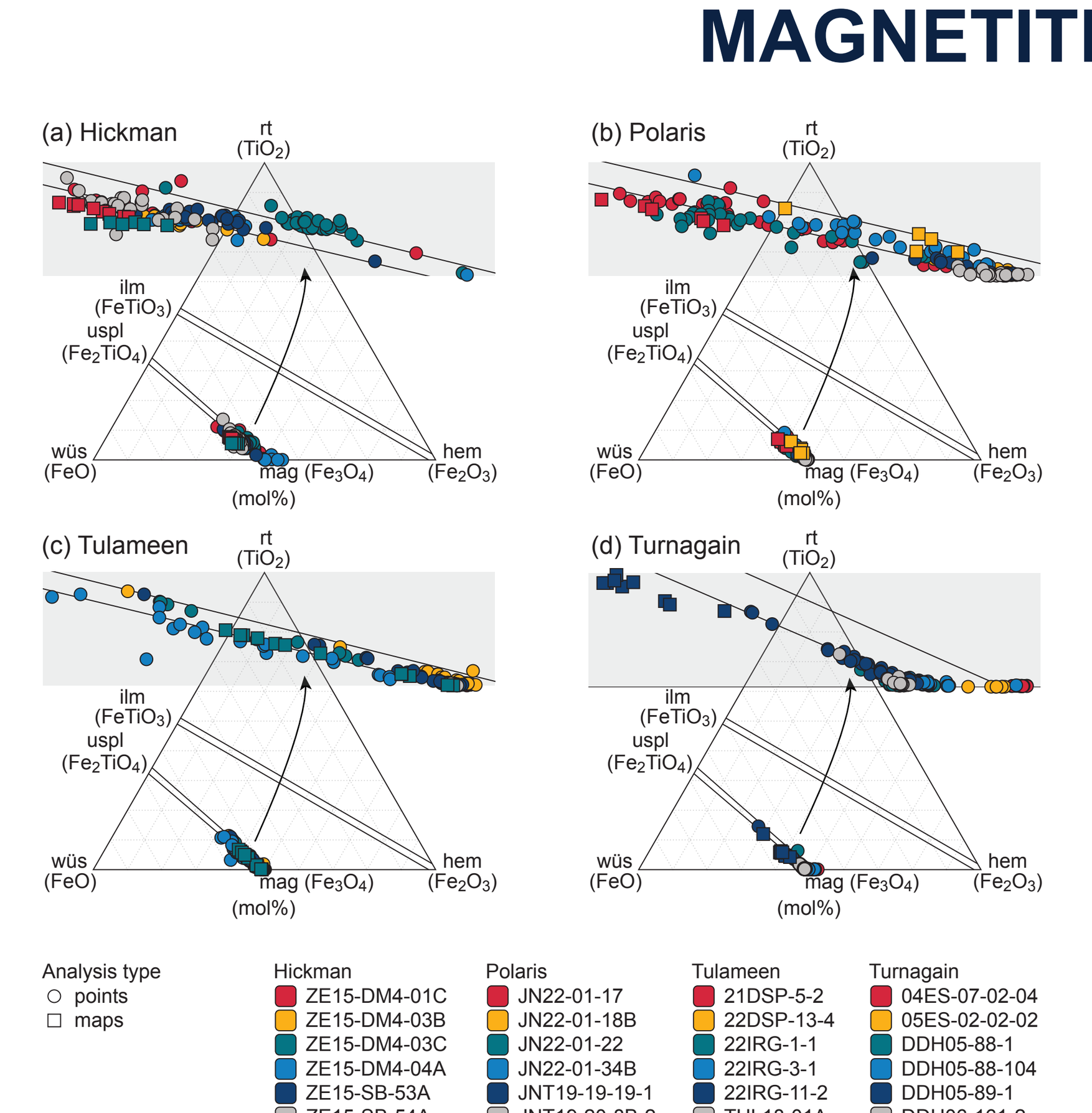

Fig. 6. Ternary FeO–Fe_2O_3–TiO_2 diagrams showing magnetite compositions analyzed by EPMA from the studied Alaskan-type intrusions. The ulvöspinel–magnetite tie line is expanded in the upper portion of each panel. Mineral abbreviations: hem (hematite), ilm (ilmenite), mag (magnetite), rt (rutile), uspl (ulvöspinel), wüs (wüstite).

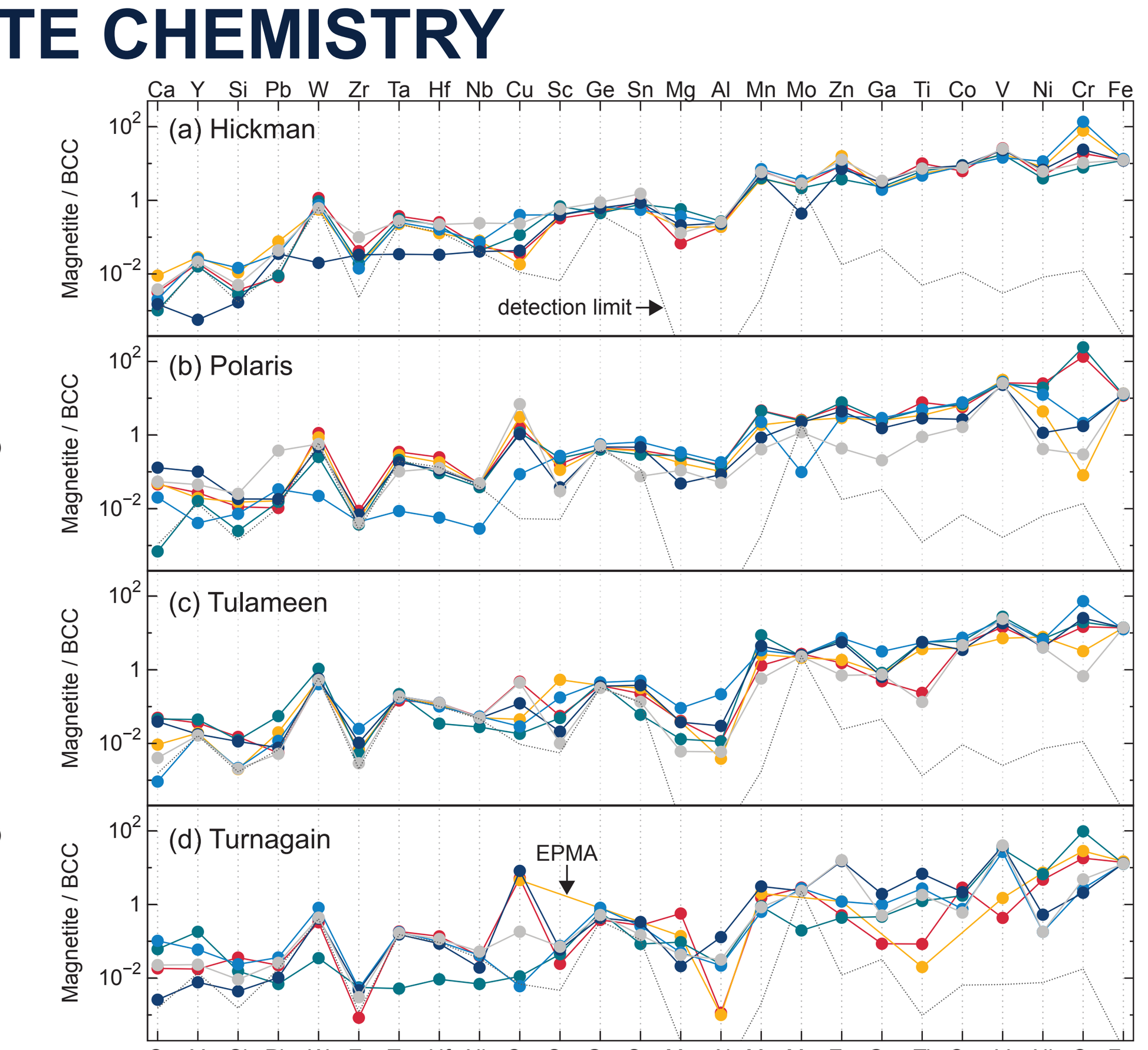

Fig. 7. Multi-element variation diagrams (modified from Dare et al., 2014a) for LA-ICP-MS major to trace element concentrations in magnetite from the studied Alaskan-type intrusions. Analyses are normalized to the bulk continental crust (BCC) using values of Rudnick & Gao (2003). Elements are ordered by magnetite/melt partition coefficient (*D*) values (Dare et al., 2012; Sievwright et al., 2017, 2020; Shepherd et al., 2022).

EFFECTS OF SUBSOLIDUS ALTERATION

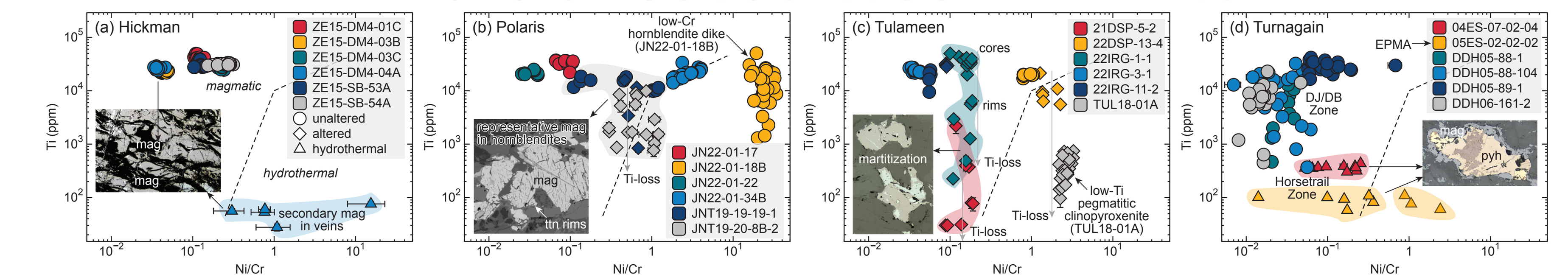

Fig. 8. Plots of Ti vs. Ni/Cr (in ppm) determined by LA-ICP-MS used to distinguish between magmatic and hydrothermal magnetite (fields as defined by Dare et al., 2014a) in the studied Alaskan-type intrusions. Secondary hydrothermal magnetite is present in Hickman (magnetite veins) and Turnagain (magnetite rims around sulfide minerals). Altered magnetite grains (e.g., martitized, disaggregated rim textures with secondary titanite (ttn), lack of exsolutions), unaltered magnetite grains, and hydrothermal magnetite are indicated by different symbols. Photomicrographs and labels are used to highlight magnetite samples with anomalous geochemistry. Compositions from Turnagain sample 05ES-02-02-02 (yellow circles) are EPMA analyses.

RECORD OF MAGMATIC FRACTIONATION

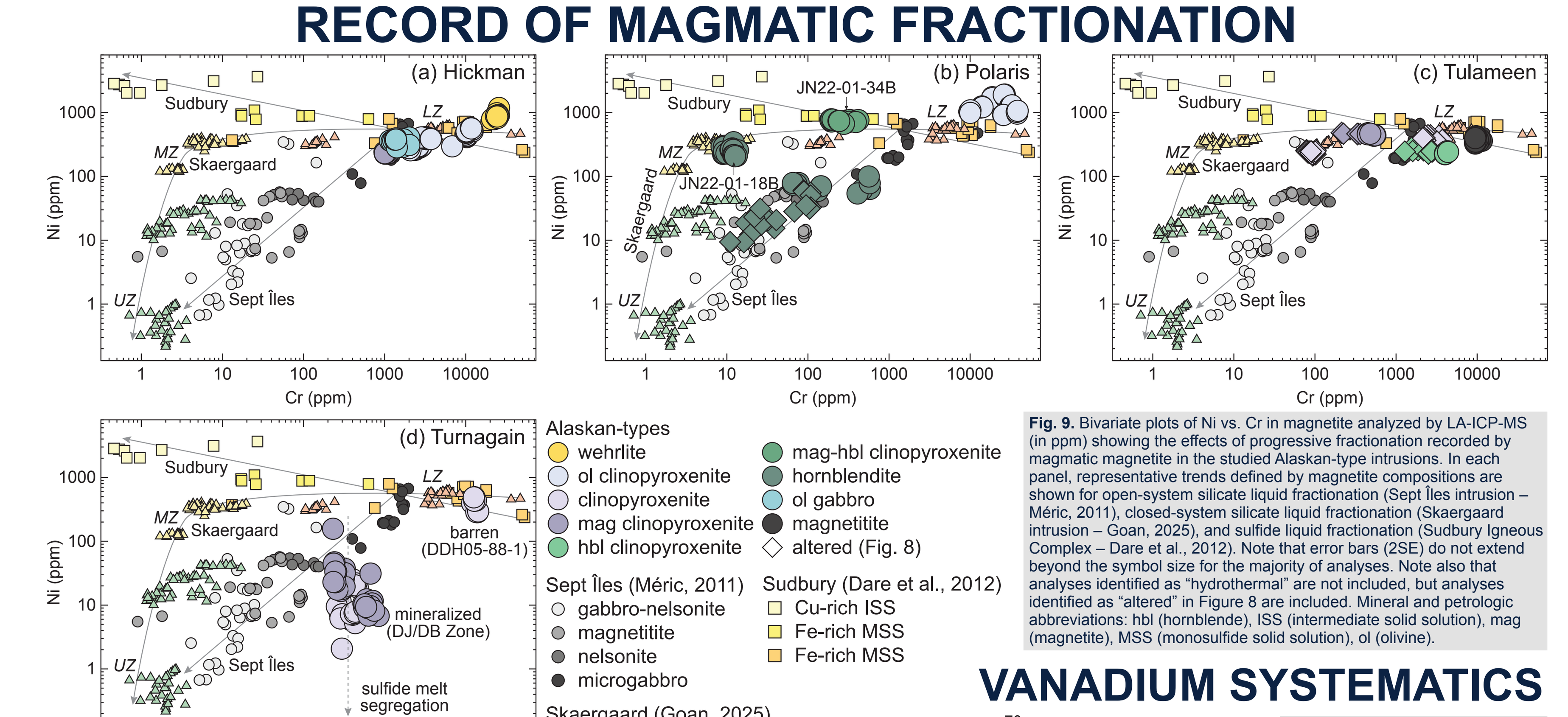

Fig. 9. Bivariate plots of Ni vs. Cr in magnetite analyzed by LA-ICP-MS (in ppm) showing the effects of progressive fractionation recorded by magmatic magnetite in the studied Alaskan-type intrusions. In each panel, representative trends defined by magnetite compositions are shown for open-system silicate liquid fractionation (Sept Îles intrusion – Méric, 2011), closed-system silicate liquid fractionation (Skaergaard intrusion – Goan, 2025), and sulfide liquid fractionation (Sudbury Igneous Complex – Dare et al., 2012). Note that error bars (2SE) do not extend beyond the symbol size for the majority of analyses. Note also that analyses identified as "hydrothermal" are not included, but analyses identified as "altered" in Figure 8 are included. Mineral and petrologic abbreviations: hbl (hornblende), ISS (intermediate solid solution), mag (magnetite), MSS (monosulfide solid solution), ol (olivine).

MINERALIZATION DISCRIMINATION DIAGRAMS

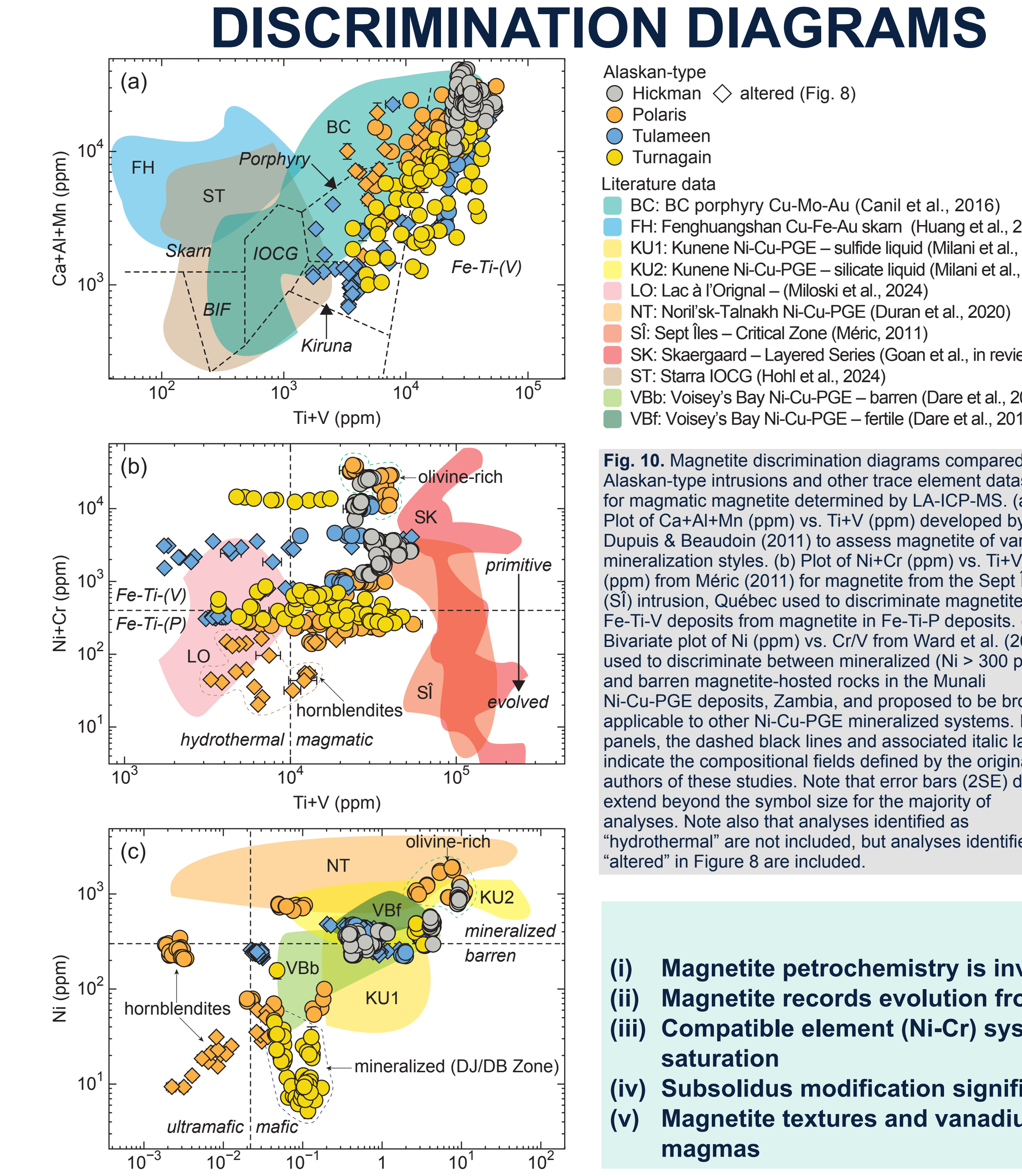

Fig. 10. Magnetite discrimination diagrams compared to Alaskan-type intrusions and other trace element datasets for magmatic magnetite determined by LA-ICP-MS. (a) Plot of Ca+Al+Mn (ppm) vs. Ti+V (ppm) developed by Dupuis & Beaudoin (2011) to assess magnetite of various mineralization styles. (b) Plot of Ni+Cr (ppm) vs. Ti+V (ppm) from Méric (2011) for magnetite from the Sept Îles (SÎ) intrusion, Québec used to discriminate magnetite from Fe-Ti-V deposits from magnetite in Fe-Ti-P deposits. (c) Bivariate plot of Ni (ppm) vs. Cr/V from Ward et al. (2018) used to discriminate between mineralized (Ni > 300 ppm) and barren magnetite-hosted rocks in the Munali Ni-Cu-PGE deposits, Zambia, and proposed to be broadly applicable to other Ni-Cu-PGE mineralized systems. In all panels, the dashed black lines and associated italic labels indicate the compositional fields defined by the original authors of these studies. Note that error bars (2SE) do not extend beyond the symbol size for the majority of analyses. Note also that analyses identified as "hydrothermal" are not included, but analyses identified as "altered" in Figure 8 are included.

VANADIUM SYSTEMATICS

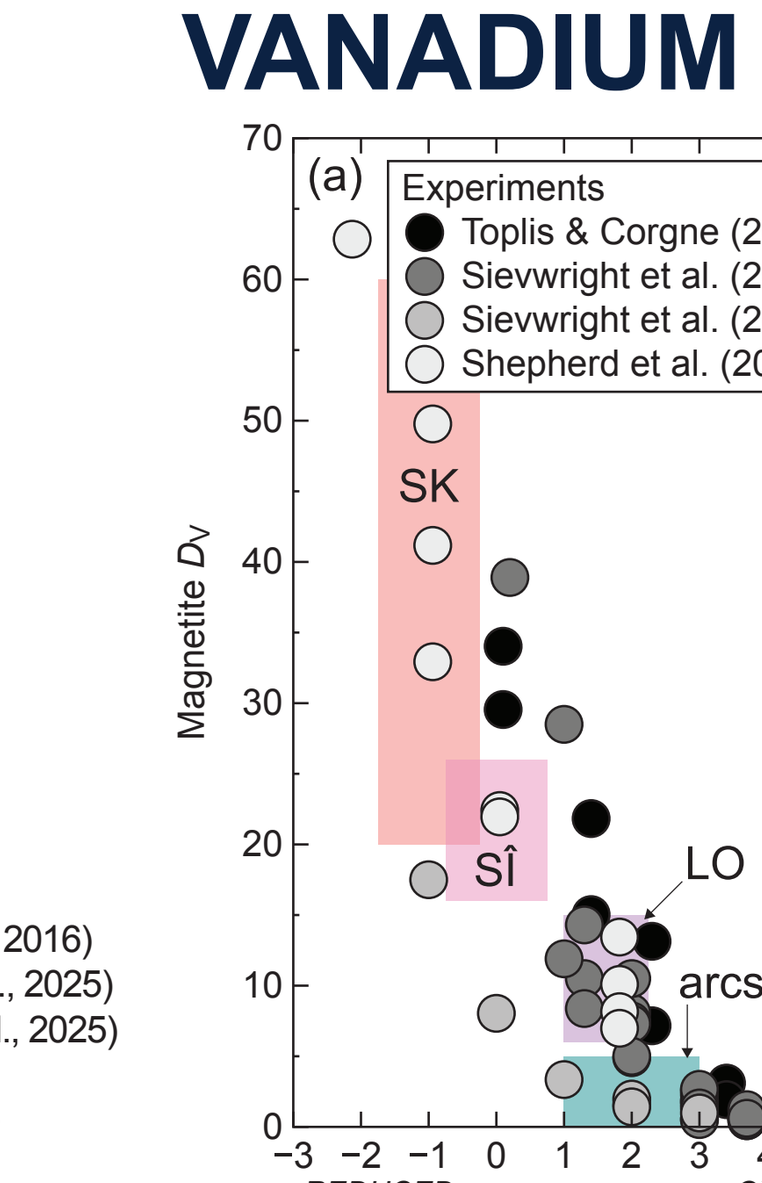

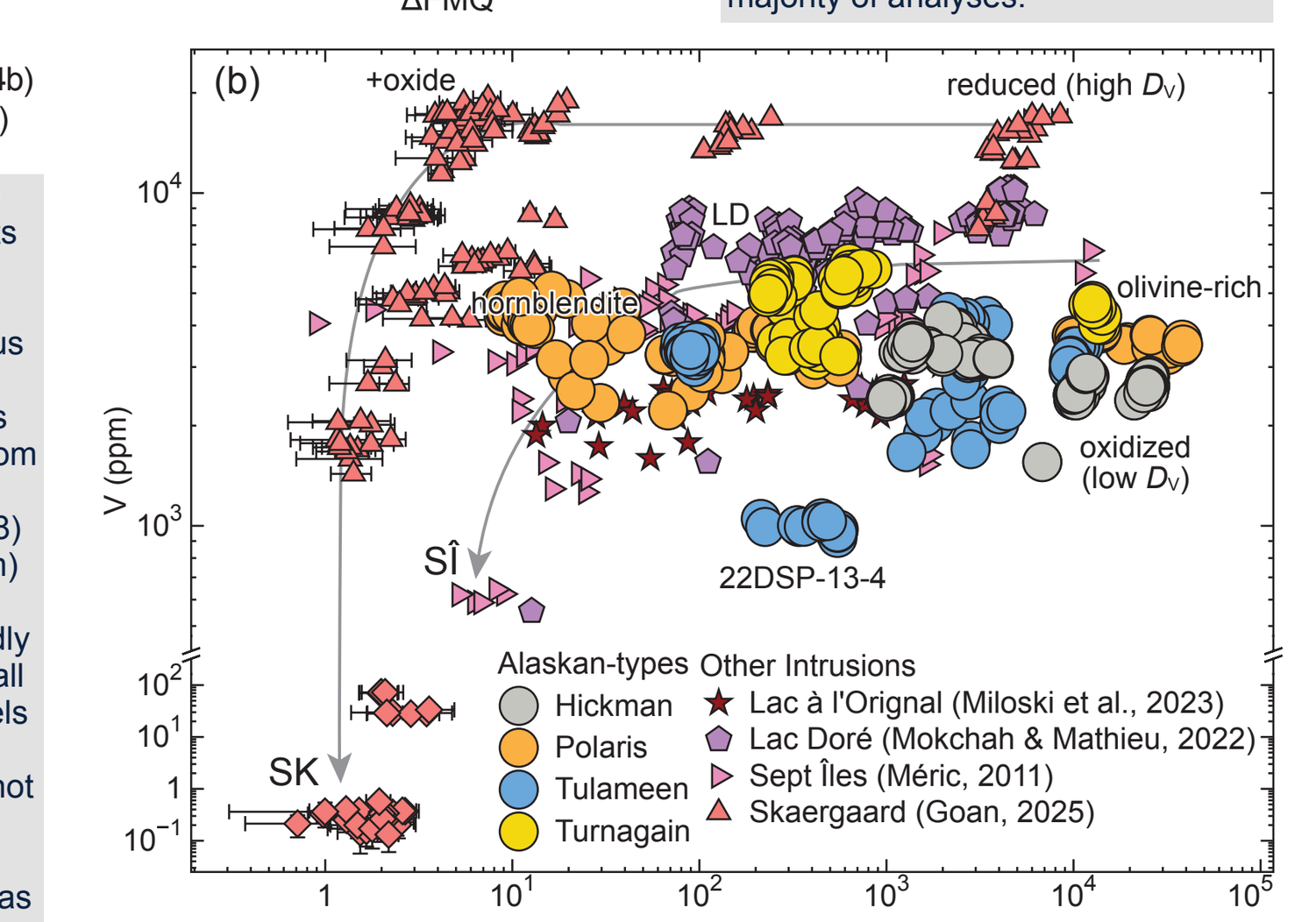

Fig. 11. Summary of vanadium (V) systematics as an oxygen fugacity (fO_2) indicator in ultramafic–mafic intrusions. (a) Partition coefficients of V (D_V) between magnetite-melt as a function of fO_2 (ΔFMQ) calculated from previous studies (Toplis & Corgne, 2002; Sievwright et al., 2017, 2020; Shepherd et al., 2022). Colored fields represent the estimated fO_2 values of several layered intrusions whose compositions are summarized in panel (b). Concentrations of V as a function of Cr in magmatic magnetite (unaltered and altered analyses included, no hydrothermal analyses) from Alaskan-type intrusions and other studied intrusions. The grey arrows indicate fractional crystallization trends as defined by Skaergaard and Sept Îles magnetite. Note the break in the y-axis and that error bars (2SE) do not extend beyond the symbol size for the majority of analyses.

SUMMARY

(i) Magnetite petrochemistry is investigated in Alaskan-type intrusions
(ii) Magnetite records evolution from primitive to fractionated magmas
(iii) Compatible element (Ni-Cr) systematics are sensitive to fractionation and sulfide saturation
(iv) Subsolidus modification significantly impacts magnetite chemistry and textures
(v) Magnetite textures and vanadium systematics are consistent with relatively oxidized magmas

ACKNOWLEDGEMENTS

We thank the research staff at the Electron Microbeam & X-ray Diffraction Facility (EMXDF) and at the Pacific Centre for Isotopic and Geochemical Research (PCIGR), particularly Dr. Anette von der Handt (EMXDF Director), Dr. Dominique Weis (PCIGR Director), and Dr. Marghaleray Amini (PCIGR Research Associate). This work was supported by Natural Sciences and Engineering Research Council of Canada (NSERC) Discovery Grants to James Scoates and a Targeted Geoscience Initiative (TGI-6) grant through the GSC to Dejan Milidragovic, including salary support to the lead author through the Research Affiliate Program (RAP). The lead author was also supported by a Society of Economic Geologists (SEG) Graduate Fellowship and an SEG Student Research Grant. This research was conducted on the traditional, ancestral, and unceded territory of the xwməθkwəyəm (Musqueam) People.

REFERENCES

Canil, D., Grondahl, C., Lacourse, T. & Pisiak, L. K. (2016). Ore Geology Reviews 72, 1116–1128. **Colpron, M. & Nelson, J. L.** (2011a). British Columbia Ministry of Energy and Mines, BCGS GeoFile 2011-11. **Dare, S. A. S.,** Barnes, S.-J., Beaudoin, G. (2012). Geochimica et Cosmochimica Acta 88, 27–50. **Dare, S. A. S.,** Barnes, S.-J., Beaudoin, G. (2012). Geochimica et Cosmochimica Acta 88, 27–50. **Dare, S. A. S.,** Barnes, S.-J., Beaudoin, G., Méric, J., Boutroy, E. & Potvin-Doucet, C. (2014a). Mineralium Deposita 49, 785–796. **Dupuis, C. & Beaudoin, G.** (2011). Miner Deposita 46, 319–335. **Duran, C. J.,** Barnes, S.-J., Mansur, E. T., Dare, S. A. S., Bédard, L. P. & Sluzhenikin, S. F. (2020). Economic Geology 115(6), 1245–1266. **Goan, I.** (2025). M.Sc. Thesis, The University of British Columbia, 545 p. **Himmelberg, G. R. & Loney, R. A.** (1995). U.S. Geological Survey Professional Paper, 1564, 1–47. **Hohl, M.,** Steadman, J. A., Cloutier, J., Barker, S. L. L., Belousov, I., Goemann, K. & Cooke, D. R. (2024). Chemical Geology 648, 23 p. **Huang, X.-W.,** Gao, J.-F., Qi, L., Meng, Y.-M., Wang, Y.-C. & Dai, Z.-H. (2016). Ore Geology Reviews 72, 746–759. **Jackson-Brown, S.** (2017). M.Sc. Thesis, The University of British Columbia, 290 p. **Méric, J.,** 2011. Internship Report, Université du Québec à Chicoutimi, Chicoutimi, Québec, 66 p. **Milani, L.,** Oosthulzen, L., Owen-Smith, T. M., Bybee, G. M., Hayes, B., Lehmann, J. & Jelsma, H. A. (2025). Mineralium Deposita 60, 551–580. **Milidragovic, D.,** Zagorevski, A. & Chapman, J. B. (2017). In: Geological Fieldwork 2016, British Columbia Ministry of Energy and Mines, British Columbia Geological Survey Paper 2017-1, 117–132. **Miloski, P.,** Dare, S., Morisset, C.-E., Davles, J. H. F. L., Perrot, M. G. & Savard, D. (2024). Mineralium Deposita 59, 519–556. **Mokchah, N. & Mathieu, L.** (2022). Journal of Petrology 53(3), 1–23. **Nixon, G. T.** (2018). In: British Columbia Ministry of Energy, Mines, and Petroleum Resources, British Columbia Geological Open File 2018-2, scale 1:20,000. **Nixon, G. T.,** Hammack, J. L., Ash, C. H., Cabri, L. J., Case, G., Connelly, J. N., Heaman, L. M., Laflamme, J. H. G., Nuttall, C., Paterson, W. P. E. & Wong, R. H. (1997). In: Ministry of Employment and Investment, British Columbia Geological Survey Bulletin 93. **Nixon, G. T.,** Milidragovic, D. & Scoates, J. S. (2019). In: Targeted Geoscience Initiative 5, Grant Program Interim Reports 2018-2019. Geological Survey of Canada Open File 8620, 49–61. **Nott, J. A.,** Milidragovic, D., Nixon, G. T. & Scoates, J. S. (2020b). In: British Columbia Ministry of Energy, Mines, and Petroleum Resources, British Columbia Geological Survey Open File 2020-04, 1:15,000 scale. **Rudnick, R. L. & Gao, S.** (2003). In: Treatise on Geochemistry 2nd Edition 3, 1–64. **Shepherd, K.,** Namur, O., Toplis, M. J., Devidal, J.-L. & Charlier, B. (2022). Contributions to Mineralogy and Petrology 177(90). **Sievwright, R. H.,** O'Neill, H. St. O., Tolley, J., Wilkinson, J. J. & Berry, A. J. (2020). Contributions to Mineralogy and Petrology 175(40), 1–21. **Sievwright, R. H.,** Wilkinson, J. J., O'Neill, H. St. O. & Berry, A. J. (2017). Contributions to Mineralogy and Petrology 172(62), 1–33. **Toplis, M. J. & Corgne, A.** (2002). Contributions to Mineralogy and Petrology 144, 22–37. **Ward, L. A.,** Holwell, D. A., Barry, T. L., Blanks, D. E. & Graham, S. D. (2018). Journal of Geochemical Exploration 188, 172–184.